

Earthquake-induced slope displacements

E. Botero J.¹ and M. P. Romo²

¹ *PhD student, Institute of Engineering, National University of Mexico*

² *Head Research Professor, Institute of Engineering, National University of Mexico*

Received: March 26, 2001; accepted: March 7, 2002

RESUMEN

Este artículo presenta un método de análisis para evaluar los desplazamientos inducidos sísmicamente en taludes. El procedimiento considera las características no lineales de los materiales, la variación espacial de la resistencia (fricción) a lo largo de la superficie potencial de falla y el efecto inercial de la cuña deslizando, la cual es considerada como un sistema flexible de múltiples grados de libertad. Los efectos potenciales son mostrados a través de casos hipotéticos por medio de varios modelos y dos sismos diferentes. El método de análisis propuesto se evalúa por medio de comparaciones con métodos existentes.

PALABRAS CLAVE: Talud, análisis sísmico, modelo discreto, cinemática.

ABSTRACT

This paper presents a finite-element analysis to evaluate earthquake-induced displacements in slopes. The procedure takes into account the nonlinear characteristics of the materials, spatial variation of strength (friction) along the potential failure surface and the inertial effects of the sliding wedge considered as a flexible multi-degree of freedom system. The potential effects are shown through hypothetical cases using two different seismic events. The model proposed in this paper is compared with other methods.

KEYWORDS: Slope, seismic analysis, discrete model, kinematics.

1. INTRODUCTION

Traditional methods for dynamic analysis of slopes have limitations in their formulations. Newmark's (1965) method assumes that the magnitude of rigid-wedge relative displacements, with respect to its support, depend on the magnitude and frequency content of the input motion. This method supposes that the security factor is equal along the entire sliding surface. The procedure developed by Chopra and Chang (1991) assumes that a rigid dam slides only if the frictional force developed at soil-dam interface is exceeded. They also considered the deformational effects of gravity dams. On the other hand they ignore higher vibration modes, because they model the problem with a single degree of freedom system. The method of Makdisi and Seed (1978) assumes that the sliding surface is completely developed according to a rigid-plastic model once the safety factor drops below one. Kramer and Smith (1997) do not consider the kinetic effects of the higher vibration modes. Rathje and Bray (1999) use the Chopra's approach but consider uniformly distributed flexible mass to model the sliding wedge.

One important aspect that the above methods do not consider is the force caused by the inertia of the soil mass that moves downward, coupled with the higher vibration modes of the descent mass. Herein, a procedure that overcomes this shortcoming is advanced.

The method proposed in this paper, model slopes with Voigt-type, viscous discrete elements can take into account the nonlinear behavior of the soil mass. The procedure is capable of computing the overall stability and earthquake-induced displacements of natural or man-made slopes. Since the analysis is carried out in the time domain, it is possible to know the behavior of a particular slope at any time during its shaking.

The importance of considering higher vibrations modes arises from the fact that multi-degree freedom systems induce inertial forces completely different than those caused by single degree systems. Indeed, at a given time the inertial forces caused by the masses in multidegree freedom systems may have opposite directions. This cannot be modeled by simple oscillators. This difference will redound in the permanent displacements computed with both approaches. Furthermore, the permanent displacements are affected by the slope vibration natural periods. Thus, if only the first natural period is considered in the analysis, the effect of the higher natural periods will be neglected. In this paper it is shown how significant is this aspect of the system response on permanent displacements.

In addition to the disadvantages previously mentioned of most available procedures, when the sliding of the soil mass is triggered, kinetic forces start playing a role in the

overall phenomenon. These kinetic forces affect, in turn, the earthquake loading vector, and consequently the inertial forces. These effects will be more notorious as the number of degrees of freedom augment.

It should be realized that when the slope is subject to large earthquake loadings, the nonlinear behavior of the soil generally modifies the overall response of the slope. Accordingly, the patterns of the kinetic and inertial forces will be changed, and so the displacements.

2. PROPOSED DYNAMIC METHOD OF ANALYSIS

Botero and Romo (2000) formulated a dynamic analysis for the sliding wedge phenomena in a slope. Their model is represented by discrete elements as shown in Figure 1.

Once the sliding surface geometry is determined, the soil mass is divided into an adequate number of discrete elements depending on the shape and height of the sliding wedge. The elements are characterized by the stiffness and damping ratios, corresponding to the soil characteristics in each layer. This could be determined with back-analyses, laboratory test or in situ test. The soil mass is lumped at the nodes to account for the inertial effects according to the mass distribution and characteristics of the slope. The boundary conditions at the model base are the failure surface friction parameters, which are determined from soil testing. The model considers static friction when the potentially sliding mass remains still and dynamic friction when sliding is triggered. The initial and subsequent inclinations of the model base are defined from the sliding surface geometry. If sliding occurs, the inclination will change throughout the seismic action. The material properties can be also modified throughout the earthquake duration, to account for the cyclic effects of soil behavior, (*i.e.*, *shear modulus degradation*).

2.1. Equilibrium equation

The acting forces on the sliding wedge (Figure 2) depend on the weight of the wedge, its stiffness, its damping and the inertia forces caused by the earthquake shaking.

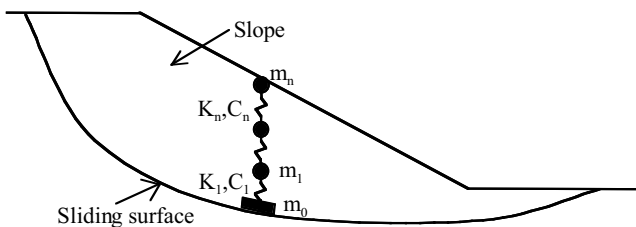


Fig. 1. Slope discrete model.

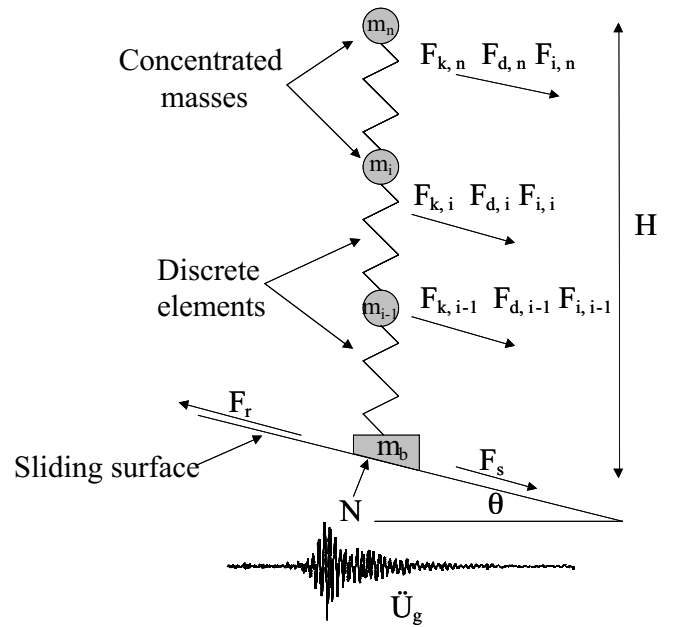


Fig. 2. Acting forces on the sliding wedge.

The internal and external forces acting in the model can be computed as follows. The resistance force F_r depends of the normal force between the lower mass and the sliding surface and is determined by Equation 1

$$F_r = N \tan(\mu), \tag{1}$$

where N is the normal force defined by Equation 2 and μ is the static coefficient of friction, when the system is sliding, the static coefficient of friction changes to the dynamic coefficient of friction. However, in this study both were considered equal.

The normal force is the resultant of the ground acceleration and gravity acceleration on the total mass acting of the system and its variation with time

$$N = M_1 [g \cos(\theta) - \ddot{U}_g \sin(\theta)], \tag{2}$$

where M_1 is the total mass of the system and is defined by Equation 3, g is the gravity acceleration, θ is the base inclination angle and \ddot{U}_g is the ground acceleration.

The total mass is given by the sum of all the masses in the system (see Figure 2)

$$M_1 = \sum_{i=1}^n m_i + m_b, \tag{3}$$

where m_i is the mass of the discrete system and m_b is the mass directly over the sliding surface.

The driving force (Equation 8) results from the active forces in the system given by Equations 4 to 7.

$$F_s = M_1 g \sin(\theta) \quad (4)$$

$$F_k = k U \quad (5)$$

$$F_d = c \dot{U} \quad (6)$$

$$F_i = m_b (\ddot{U}_g + \ddot{U}_0) \quad (7)$$

$$F_a = F_s + F_k + F_d + F_i, \quad (8)$$

where F_s is the shear force at the model base due to the overlying weight. F_k is the stiffness force due to relative displacement between contiguous nodes and k is the element stiffness. U is the relative displacement of a node with respect to the base. F_d is the damping force due to the relative velocity between the node and the base and c is the element damping. \dot{U} is the relative velocity of the node with respect to the base, and F_i is the inertial force due to mass m_i times $(\ddot{U}_0 + \ddot{U}_g)$. Here \ddot{U}_0 is the acceleration of the system when it slides at its base and F_a is the induced force by the excitation (driving force).

Taking Equations 4 to 7 and replacing them in Equation 9, we obtain:

$$F_a = M_1 g \sin(\theta) + k u + c \dot{U} - m_b (\ddot{U}_g + \ddot{U}_0). \quad (9)$$

During the seismic excitation, the slope equilibrium is evaluated by means of Equations 1 and 8. When $F_a > F_r$ occur permanent displacements that keep on increasing until the driving force drops below the resisting force.

2.2. Equation of movement

The response of each node, when the system does not slide, can be computed with the following equation of motion:

$$[M](\ddot{U}) + [C](\dot{U}) + [K](U) = -M_1 (\ddot{U}_g \cos(\theta)), \quad (10)$$

where M is the mass matrix, \ddot{U} is the base relative acceleration vector, C is the damping matrix, \dot{U} is the base relative velocity vector, K is the stiffness matrix and U is the base relative displacement vector.

When the system slides, the equilibrium at the sliding interface is established to compute the kinetic acceleration. The equation of motion for this condition is given by

$$M_1 \ddot{U}_c = -\mu_c [M_1 g \cos(\theta) - M_1 \ddot{U}_g \sin(\theta)] - \sum_{i=1}^n \ddot{a}_i m_i - M_1 \ddot{U}_g \cos(\theta), \quad (11)$$

where \ddot{a}_i is the relative acceleration, of node i , parallel to the sliding surface, \ddot{U}_c is the kinetic acceleration, μ_c is the kinetic friction coefficient and n is the number elements. The kinetic acceleration is computed with Equation 12

$$\ddot{U}_c = -\mu_c [g \cos(\theta) - \ddot{U}_g \sin(\theta)] - \frac{1}{M_1} \sum_{i=1}^n \ddot{U}_i m_i - \ddot{U}_g \cos(\theta). \quad (12)$$

When the system is sliding, the equation of motion of the full system is

$$[M](\ddot{U}) + [C](\dot{U}) + [K](U) = -M_1 (\ddot{U}_c + \ddot{U}_g \cos(\theta)). \quad (13)$$

2.3. Dynamic model of the materials behavior

The nonlinear behavior of the materials is computed with the angular deformation between nodes (Equation 14) and a Masing-type model (Romo, 1995). The angular deformation is:

$$\gamma = \frac{U_i - U_{i-1}}{2H}, \quad (14)$$

where U_i is the displacement of the node i , U_{i-1} is the displacement of node $i-1$ and H is the separation between them. The shear modulus and damping ratio curves can be expressed as:

$$\frac{G(\gamma)}{G_{max}} = [1 - H(\gamma)], \quad (15)$$

where $G(\gamma)$ is the shear modulus for any deformation and G_{max} is the maximum shear modulus.

$$H(\gamma) = \left[\frac{\left(\frac{\gamma}{\gamma_r} \right)^{2B}}{1 + \left(\frac{\gamma}{\gamma_r} \right)^{2B}} \right]^A, \quad (16)$$

where γ_r is a reference deformation, and A and B are parameters dependent of the plasticity index. The parameter A could have values between 0.56 - 1.0 and parameter B varies from 0.2 to 0.86.

The capacity of the system to dissipate energy can be computed with the following equation:

$$\lambda = (\lambda_{max} - \lambda_{min}) (H(\gamma)) + \lambda_{min}, \quad (17)$$

where λ is the damping ratio for deformation γ , λ_{max} is the maximum value of λ that can be reached before soil fails under dynamic load and λ_{min} is the minimum value of λ .

3. MODEL VALIDATION

The model was compared with that proposed by Bray *et al.* (1995). The results for slope models with heights of 16 m, 32 m, 44 m and 60 m are compared in Figure 3. It may be seen that both approaches yield similar results.

To evaluate the model capabilities to compute permanent displacements in a slope as a function of the period it was compared with the model proposed by Kramer *et al.* (1997). The 1989 Loma Prieta earthquake acceleration record was used as input motion. Again, it may be seen that the proposed model yields similar results to those produced by Kramer *et al.*'s model. The results are shown in Figure 4.

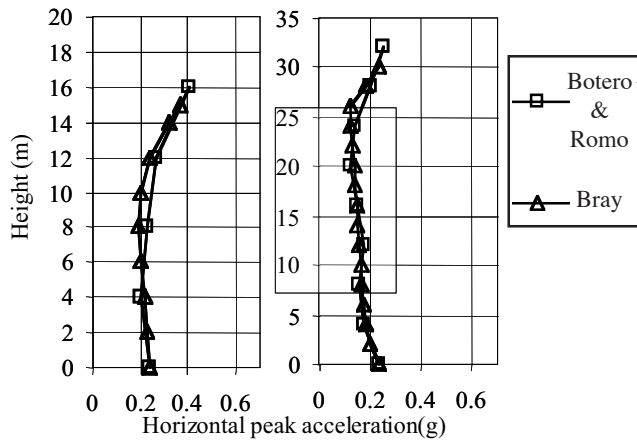


Fig. 3. Comparison between Bray *et al.*'s and Botero and Romo's methods.

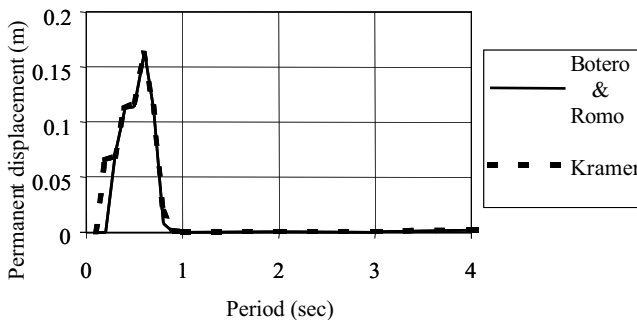


Fig. 4. Comparison between Kramer *et al.*'s and Botero and Romo's methods.

4. APPLICATION CASE

The slope of the Figure 1 was analyzed in order to show the effect and the influence of the kinetic forces and the number of degrees of freedom used to discretize the slope, when mass sliding is triggered, on the magnitude of earthquake-induced permanent displacements. The input motions were the accelerographs recorded at SCT site (which is located within the soft sediment zone where heavy damage was caused in Mexico City) during the Michoacán earthquake of September 19, 1985 and at Yerbabuena Island in San Francisco Bay during the 1989 Loma Prieta earthquake. The fundamental periods of these accelerograms are 2.35 s and 0.62 s, respectively. This section intended to evaluate the effects of the natural periods of the slopes and the earthquakes characteristics on the permanent displacements, considering the condition of a soil mass sliding. The height of the slope was 75 m. The sliding mass was concentrated at each node, and the inclination of the sliding surface was 5°. The slope characteristics were kept equal for the three models for each earthquake.

4.1. Effect of the slope's freedom degrees

The traditional methods only consider one degree of freedom systems. To evaluate the potential effect of slope flexibility (considering more than one degree of freedom) on earthquake-induced displacements, three models having one, two and three degrees of freedom were considered. The results of the analyses were interpreted making use of the displacement spectrum proposed by Kramer *et al.* (1997). The ordinates of this spectrum correspond to the permanent displacements accumulated throughout the excitation, for different values of the slope natural period. This shows the influence of the slope flexibility on the permanent displacements induced by the given seismic event. The spectra computed for the slope discretized using one, two and three degrees of freedom for the Michoacán and Loma Prieta earthquakes are depicted in Figure 5.

It may be seen that all spectra are alike in the neighborhood of the earthquake fundamental period, and that the maximum permanent displacements occur at the earthquake fundamental period. For the Michoacán earthquake, the slope discretized with three degrees of freedom accumulates more displacement compared with the slopes having one and two degrees of freedom, that those developed for about the same maximum displacement for the Loma Prieta earthquake. It may be seen that the systems with two and three degrees of freedom, are similar and their displacement magnitudes are lower than for the one-degree of freedom system. These results are revealing because they show the potential effects of the higher vibration modes on the permanent displacements. Also, they show that the frequency content of the input motions can affect appreciably the magnitude of the slope per-

manent displacements. To give an idea of how these displacements develop throughout the action of the seismic event, time-displacement plots are presented in Figure 6 for the cases of the slope having $T= 2.20$ s (Michoacán earthquake) and $T= 0.62$ s (Loma Prieta earthquake). These periods correspond to the condition where the maximum values of permanent displacements were developed.

The results indicate that the permanent displacements for the three models for Michoacán earthquake starts developing about the same time and with similar magnitudes, but the increments depend on the numbers of degrees of freedom. Similar patterns are observed for the Loma Prieta earthquake. These findings demonstrate that when slope flexibil-

ity is modeled, considering more than one degree of freedom, the response of the slope and thus the induced permanent displacements depend on the frequency content of the input motion.

4.2. Effect of kinetic acceleration

In this case, the corresponding term in Equation 13 was activated. The displacement spectra are presented in Figure 7 for the three considered models.

Comparing Figures 7 and 5, it becomes evident that the smoothness of the spectral curves is lost in the models where kinetic effects are accounted for. In the case of the slopes

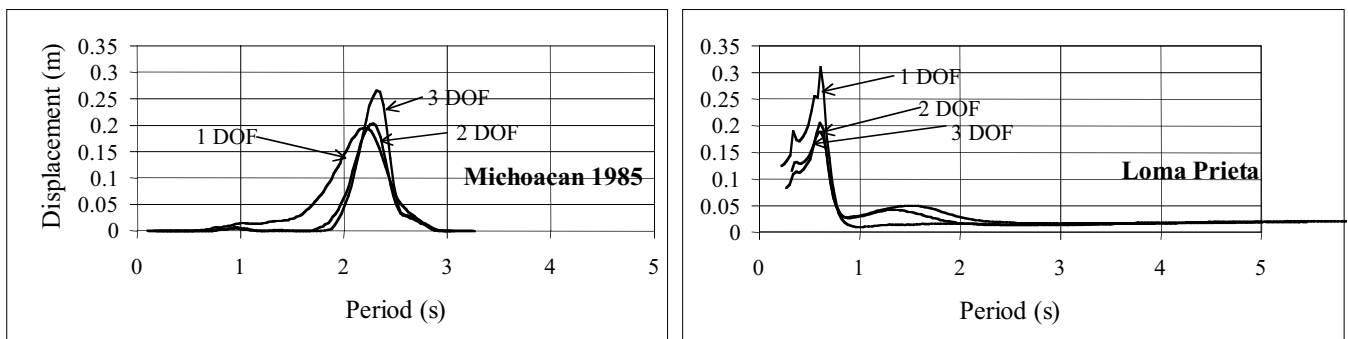


Fig. 5. Multi-degree of freedom models without inertial effect.

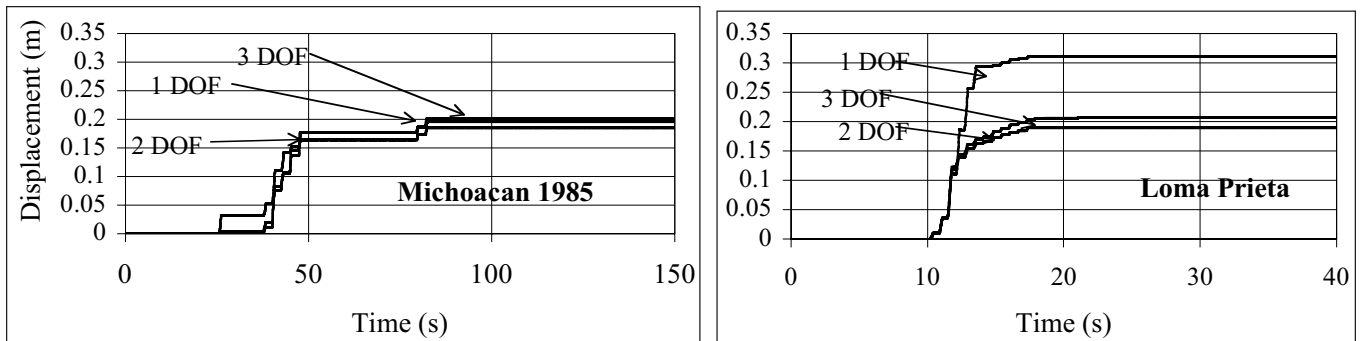


Fig. 6. Slope displacements with no inertial effects included.

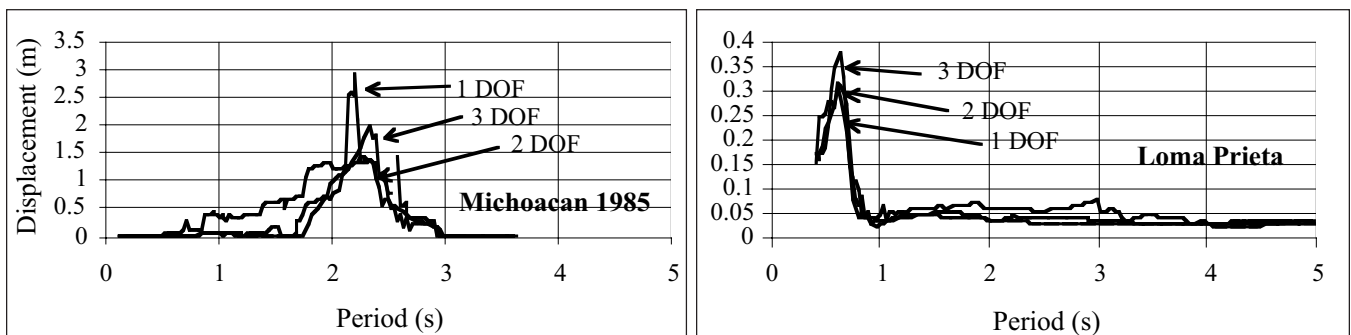


Fig. 7. Multidegree of freedom models with inertial effect.

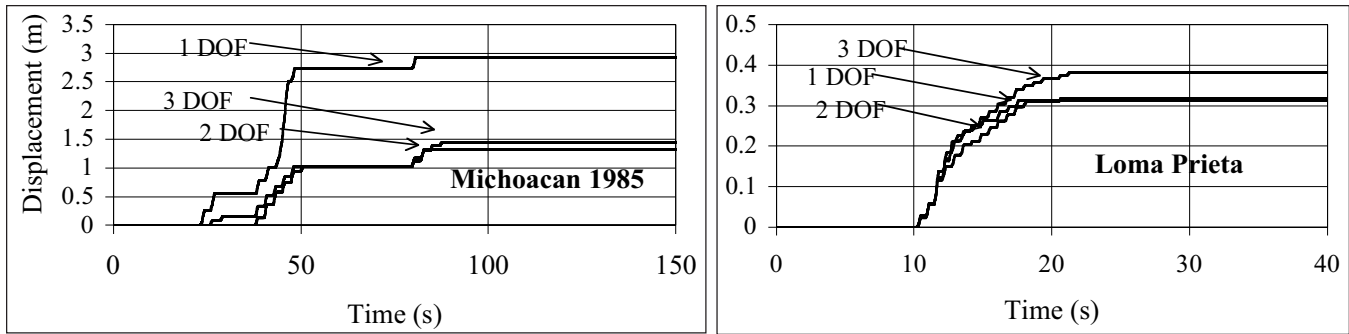


Fig. 8. Base displacement in a multi-degree of freedom model with inertial effects.

with the Michoacán earthquake data a much larger permanent movements were developed. However, the slopes excited by the Loma Prieta earthquake did not show a significant increase in displacements due to inertial effects. The time-displacement curves of Figures 6 and 8 show that the displacement patterns throughout the action of the seismic events are modified when the kinetic forces are considered for the $T=2.20$ s and $T=0.62$ s fundamental periods of the Michoacán and Loma Prieta earthquakes, respectively.

For the Michoacán earthquake it is seen that the kinetic acceleration effect shows up at instant times for each of the models. At this point, it may be argued that the differences on the time-displacement patterns observed in the results given above, are mainly due to the variations in the magnitude and direction of the inertia forces developed at each of the degrees of freedom. Now, depending on the earthquake frequency content these inertial forces may partially compensate between them or superimpose.

The results also point that as the earthquake intensity increases, the kinetic effect becomes more significant. Furthermore, the consideration of the kinetics in the dynamic response of the slopes may cause instabilities of the solution as depicted in the Figure 7, for the case of three degrees of freedom system excited by the Michoacán earthquake. This suggests that the coupling effect of kinetics and multi-degree of freedom discretizations may lead to inelastic responses of the slopes. Thus, a new field of study of the response of earth structures should be envisioned.

5. CONCLUSIONS

This paper revisits Newmark's model to evaluate earthquake-induced permanent movements in slopes. It attempts to account more explicitly for the effects of slope flexibility and kinematic forces caused by a sliding mass.

The results indicate that higher vibration modes of the slopes may increase or decrease their permanent movements

as compared with the current procedures that include the flexibility of the slope modeled by a one-degree-of-freedom system. This influence is amplified when the kinetic forces are considered. Furthermore, this additional loading modify the displacement patterns, which can be critical when the slopes of an embankment are designed.

BIBLIOGRAPHY

- BOTERO, E. and M. P. ROMO, 1999. Dynamic behavior of solid waste landfills. Internal Report, Institute of Engineering, National University of Mexico, Mexico. (in Spanish).
- BOTERO, E. and M. P. ROMO, 2000. Seismic analysis of solid waste landfills. XX National Meeting of Soil Mechanics, 2, 231-240 Oaxaca, Mexico.(in Spanish).
- BRAY, J., G. LEONARDS, P. REPETTO and J. BYRNE, 1995. Seismic stability procedures for solid waste landfills. *J. Geotech. Geoenviron. Eng., ASCE*, 121 (2), 139-151.
- CHOPRA, A. K. and L. ZHANG, 1991. Earthquake-induced base sliding of concrete gravity dams. *J. Struc. Eng. ASCE*, 117 (12), 3698-3719.
- KRAMER, S. L. and M. W. SMITH, 1997. Modified Newmark model for seismic displacements of the compliant slopes. *J. Geotech. Eng., ASCE*, 123 (7), 635-644.
- MAKDISI, F. I. and H. B. SEED, 1978. Simplified procedure for estimating dam and embankment earthquake-induced deformations. *J. Geotech. Eng., ASCE*, 104 (7), 849-867.
- NEWMARK, N. M. 1965. Effects of earthquakes on dams and embankments. *Geotechnique*. 15 (2), 139-160.

RATHJE, E. M. and J. D. BRAY, 1999. An examination of simplified earthquake-induced displacement procedures for earth structures. *Canadian Geotech. J., Ottawa, 36*, 72-87.

ROMO, M. P. 1995. Clay Behavior, ground response and soil-structure interaction; studies in Mexico City. Third International Conference on Recent Advances in Geotechnical Earthquake Engineering and Soil Dynamics. St. Louis Missouri, Vol. 2, 1039.

E. Botero¹ J. and M. P. Romo²

¹ PhD student, Institute of Engineering, National University of Mexico, EboteroJ@iingen.unam.mx

² Head Research Professor. Institute of Engineering, National University of Mexico. mromo@pumas.iingen.unam.mx